Particle Mass Measurements and Strong Interaction Studies with Exotic Atoms using X-ray Crystal Spectrometer at the Fermilab Main Injector

(Updated Proposal)

March 31, 2001

A.S.Denisov, Yu.M.Ivanov*, A.A.Kotov, L.P.Lapina, S.Yu.Nesterov,
A.A. Petrunin, A.I.Schetkovsky, V.V.Skorobogatov, V.M.Suvorov
Petersburg Nuclear Physics Institute, Gatchina 188300, Russia

D.Armstrong**, M.Eckhause, J.Kane, R.Welsh
College of William and Mary, P.O.Box 8795, Williamsburg, Virginia 23187, USA

G.Borchert
Institut fur Kernphysik, Forschungszentrum Julich, D-52425 Julich, Germany

Abstract

---

* spokesperson, e-address: yumi@rec03.pnpi.spb.ru, yumi@fnal.gov
tel: 7-81271-32046 ; fax: 7-81271-37196
** deputy spokesperson, e-address: armd@physics.wm.edu
tel: 1-757-221-3513 ; fax: 1-757-221-3540

Precision measurements of X-ray transitions in μ, π, K, $\overline{p}$, Σ, Ξ and Ω atoms of light elements with crystal spectrometer at the FNAL Main Injector are proposed with aim to improve particle masses including muon neutrino mass limit, to improve hyperon magnetic moments, to measure, at first, hyperon-nucleus spin-orbit interaction, to search for Σ^- n hypernucleus and, if exists, to measure its binding energy.

Since April, 1999 when the initial proposal was submitted to FNAL we have developed technology for preparing toroidal surfaces and technique for optical contacting crystal plates with these surfaces. It enables us to design and construct the crystal spectrometer of the reflection type with a double focusing instead of the transmission spectrometer, as suggested in the initial proposal. With a new spectrometer it will be possible to use the relatively thin beam targets (2 cm instead of 20 cm) without any essential losses in event's counting rates and with an improved effect-to-background ratio. Simulations for double focusing scheme are presented, measurements and setup features are discussed.

Contents

1. Introduction

Negatively charged particle (μ^-, π^-, K^-, $\bar{p}$, Σ^-, Ξ^-, Ω^-) when stopped in matter produces exotic atom emitting X-rays which carry information on particle mass, spin, magnetic moment, electric quadrupole moment, and interaction with nucleus.

The intensive 120 GeV proton beam of the FNAL Main Injector provides new possibilities for researches with exotic atoms which are described in the proposed experiment.

Goals of the experiment are:

- to measure π^- and K^- masses with precision of several parts per million (ppm) or better to solve previous discrepancies and improve muon neutrino mass limit;
- to improve Σ^-, and, possibly, Ξ^-, Ω^- hyperon masses by one to two orders of magnitude;
- to improve magnetic moment of Σ^- hyperon by a factor of 2, and, possibly, to measure, at first, spin and quadrupole moment of the Ω^- hyperon;
- to measure, at first, spin-orbit strong Σ^- nucleus interaction to test quark structure effects;
- to search for lightest hypernucleus $\Sigma^- n$, and, if exists, to measure its binding energy.

To reach the goals we propose to build a crystal-diffraction facility for studying exotic atom's X-rays at the FNAL Main Injector. The facility should provide necessary instrumental accuracy for particle mass measurements and sufficient resolution for spin and magnetic moment studies.

To increase counting rate it is proposed to measure exotic atom's X-rays directly from target irradiated by the 120 GeV proton beam (Fig.1, Fig.2), that ensures high efficiency of the capturing onto atomic levels the particles having short lifetime.

The approach was successfully used at IHEP (Protvino) [1,2] for measuring K^- and Σ^- atomic X-rays with 70 GeV proton beam, and, more previously, at PNPI (Gatchina) [3], Caltech [4], Nevis [5], and PSI [6] for pionic atom's studies with 0.6 – 1 GeV proton beams.

Since April, 1999 when our initial proposal was submitted to FNAL we have developed a technology for preparing toroidal surfaces and technique for optical contacting crystal plates with these surfaces. It enables us to design and construct the crystal spectrometer of the reflection type with a double focusing (Fig.3)instead of the transmission spectrometer, as in the initial proposal. With a new spectrometer it will be possible to use the relatively thin beam targets (2 cm instead of 20 cm) without any essential losses in event's counting rates and with an improved effect-to-background ratio.

Below we present simulations of possible measurements and discuss setup features.

2. Physics with Exotic Atoms at the FNAL Main Injector

2.1 π^- Mass

Exotic atom is a hydrogenic atom with level energies proportional, in good approximation, to the orbit particle mass, so the latter can be obtained from precise measurements of X-ray energies emitted by exotic atoms. This requires to fit a calculated transition energy to measured one using mass as a parameter. As a rule, precise calculation of transition energy is provided by a numerical integration of relativistic equation with taking into account polarisation of vacuum, nuclear size, electron screening, and some other effects.

The current π^- mass value [7]

$$m_{\pi^-} = 139.57018 \pm 0.00035 \text{ MeV/c}^2 \text{ (2.5 ppm)}$$

is based upon X-ray wavelength measurements for 4f-3d transition in π-atomic magnesium [8] and for 5g-4f transition in pionic nitrogen [9] , both were made at the PSI.

In the first experiment data analysis gave two solutions for mass with equal probabilities. The difference between these solutions is equal to 2.13 keV/c^2, or 15.3 ppm, that is about 6 times larger

than solution's error which is equal to 0.35 keV/c^2 (2.5 ppm) . The choice of Particle Data Group from the two solutions was made in such a way as to reach, assuming CPT invariance, a consistency with a positive mass-squared for the muon neutrino given by the precise measurement of muon momentum for the pion decay at rest [10], a contradictory solution was rejected from fit.

The ambiguity of π^- mass from experiment [8] is related with accounting for electron screening effect in the measured transition energy. As known, the transition should have three components corresponding to three possible states of electronic shell at the moment of emitting photon: state of full ionisation, state with one, and state with two K-electrons. The problem consists in the uncertainty of component intensities, so the electron screening correction for unresolved transitions has an ambiguity comparable with the splitting magnitude. In the experiment [8], the line splitting due to one K-electron was equal to about 0.5 eV (19 ppm with respect to transition energy of 25.9 keV) and the spectrometer resolution was only 0.93 eV. The insufficiency of resolving power led to an ambiguity of 15 ppm in pion mass.

In the second experiment [9] the pionic mass was measured with an error 0.53 keV/c^2 (4.6 ppm). The ambiguity from electron screening effect in this experiment was suppressed by using a low pressure gaseous target (according to cascade calculations a line structure from gaseous target has one dominant component which corresponds to full ionisation of the electronic shell). Disadvantage of the gaseous target is a low counting rate which results in a larger statistical error.

Since the pion mass value has important consequences in particle physics, new precise measurements with accuracy of about [8], or better, are necessary. From this point of view a proposed crystal facility at the Main Injector can provide excelent experimental conditions for measurements with pionic atoms.

We made simulation of possible measurement of the 5f-3d transition in pionic oxygen having energy of 16.77 keV and splittings of 1.2 eV and 0.8 eV between components. The result of simulation is shown in Fig.4. The intensity ratio of components was taken to be 30:10:1 [8], the energy resolution was estimated to be 0.35 eV for silicon crystal with quasimosaics of about 3 arcsec. From the figure one can see that splittings ΔE and ΔE_1 between neighbouring components are different, and the difference between them is measurable. It means that in case of third component appearing to be weaker than predicted, none the less the unambigous component's identification and, respectively, the π^- mass determination can be made using only other two components. The estimated statistical error for several hours exposition is less than 1 ppm, therefore an accuracy of experiment will be determined, in practice, by an instrumental and calibration errors only.

Charged pion mass is used for calculation of "laboratory" upper limit on the ν_μ mass from the end-point energy of pion decay at rest. This method consists of searching for kinematic effects that result from nonzero neutrino mass and does not depend upon the existence of lepton-flavor violation (as in case of neutrino oscillation method).

At present the upper limit on the ν_μ mass is equal to $m_{\nu\mu} < 0.19$ Mev/c^2 [7]. It comes from energy-momentum conservation in π^+ decay at rest, where three measured values enter: the pion mass (assuming CPT theorem the π^- mass, which is more precise, is taken instead of the π^+ mass), the muon mass, and the muon momentum

$$m_{\nu_\mu}^2 = m_{\pi^-}^2 + m_{\mu^+}^2 - 2m_{\pi^-} \cdot \sqrt{p_{\mu^+}^2 + m_{\mu^+}^2} \,.$$

The derivatives of squared neutrino mass on $m_{\pi-}$, $m_{\mu+}$, $p_{\mu+}$ are approximately the same and this circumstance leads to equal sensitivity of neutrino mass from absolute errors of these three values. The errors are equal to 0.35 keV, 0.034 keV, and 0.12 keV, respectively [7]. Since the error of π^- mass is about 3 times larger than other errors, it completely determines the neutrino mass limit obtained from the equation. So the improvement of charged pion mass improves restriction on the muon neutrino mass and checks muon momentum measurement.

2.2 K^- Mass

The current K^- mass value

$$m_{K^-} = 493.677 \pm 0.013 \text{ MeV/c}^2 \text{ (26.3 ppm)} \qquad [7]$$

is the average of the six charged kaon mass measurements with very large scale factor of 2.4 for error, what indicates a serious disagreement between different input data.

The main discrepancy is between the two most recent results:

$$m_{K^-} = 493.696 \pm 0.007 \text{ MeV/c}^2 \text{ (14.2 ppm)} \quad [1], \text{ and}$$

$$m_{K^-} = 493.636 \pm 0.011 \text{ MeV/c}^2 \text{ (22 ppm)} \quad [11]$$

both of which are determined from measurements of X-ray energies of kaonic atoms. Their average has $\chi^2 = 21.2$ for 1 D.F. which corres-ponds to 0.004% probability [7]. The relative difference between these two experiments is about of 120 ppm and originates from measurements of 9-8 transition in kaonic lead (at BNL, [11]) and 4f-3d transition in kaonic carbon (at IHEP, [1]).

To clarify situation with kaonic mass we propose to measure with a high accuracy the 4f-3d transition in kaonic carbon and the 5g-4f transition in kaonic oxygen. The result of simulation for 4f-3d transition in kaonic carbon is shown in Fig. 5, for oxygen the result is similar (Fig.6). The estimated exposition for each of these transitions does not exceed ten hours providing statistical error better than 1 ppm.

The improvement of charged K-mass may contribute to muon neutrino mass problem. As pointed out by different authors [12-15], the three-body kaon decays are more sensitive to the muon neutrino mass, than two-body pion decay, due to linear dependence of neutrino mass on muon end-point energy. In case of $K^+_{\mu 3}$ decay the kinematic equation is:

$$m_{\nu_\mu} = \frac{m_{K^-}}{m_{\pi^0}} \cdot \left(\frac{m_{K^-}^2 + m_{\mu^+}^2 - m_{\pi^0}^2}{2m_{K^-}} - E_0 \right).$$

where E_0 is the end-point energy of μ^+, and K^- mass is put instead of K^+ mass due to CPT conservation.

From equation the muon neutrino mass limit depends on the uncertainties of $m_{\mu+}$, $m_{\pi 0}$, m_{K^-} and E_0 in proportion to the corresponding derivatives:

$$\frac{\partial m_{\nu_\mu}}{\partial m_{\mu^+}} = \frac{m_{\mu^+}}{m_{\pi^0}} = 0.78,$$

$$\frac{\partial m_{\nu_\mu}}{\partial m_{\pi^0}} = -\frac{m_{\pi^0} + m_{\nu_\mu}}{m_{\pi^0}} \approx -1.00,$$

$$\frac{\partial m_{\nu_\mu}}{\partial m_{K^-}} = \frac{m_{K^-} - E_0}{m_{\pi^0}} = 1.88,$$

$$\frac{\partial m_{\nu_\mu}}{\partial E_0} = -\frac{m_{K^-}}{m_{\pi^0}} = -3.66.$$

The $m_{\mu+}$, $m_{\pi 0}$ and m_{K^-} mass uncertainties are equal to 0.034 keV/c^2, 0.6 keV/c^2 and 60 keV/c^2, respectively (for kaon mass uncertainty it was taken a difference between low-Z and high-Z

measurements due to systematic nature of discrepancy). In result, the contribution from meson masses to neutrino mass uncertainty is equal to

$$\Delta_{\mu\pi K} = \sqrt{(0.78 \cdot \Delta m_{\mu})^2 + (1.00 \cdot \Delta m_{\pi^0})^2 + (1.88 \cdot \Delta m_K)^2} = 113 \text{ keV/c}^2,$$

which is comparable with adopted upper limit for muon neutrino mass (190 keV/c^2).

If the charged K-mass will be measured with the precision of several ppm, as we propose, the meson mass contribution will be reduced to 2–3 keV that will provide a principal possibility to improve current muon neutrino mass limit by about two orders of magnitude by measuring the end-point energy of μ^+ in $K^+_{\mu 3}$ – decay at rest. We suppose further studies of $K^+_{\mu 3}$ – decay at BNL, KEK, and DAFNE appear to be quite promising to measure end-point energy with high accuracy.

2.3 Σ^- Mass and Magnetic Moment

If orbit particle has spin S, magnetic moment $\mu = gS(e\hbar/2mc^2)$, and electric quadrupole moment Q, its energy level with quantum numbers n and ℓ has a fine structure which is described by the expression [16]:

$$E^{fine}_{n,l} = E_{n,l} + \frac{(Z\alpha)^4 mc^2}{2n^3 l(l+1)(2l+1)}[(g-1)X + Q\frac{3X(X+1) - 4l(l+1)S(S+1)}{3(2l-1)(2l+3)}],$$

where $X = j(j+1) - l(l+1) - S(S+1)$. By measuring the fine structure splittings together with a transition energy the particle spin and moments can be determined simultaneously with the particle mass. We propose to use this method for Σ^- mass and magnetic moment measurements.

Current world averages of Σ^- mass and magnetic moment [7] are equal to

$$m_{\Sigma^-} = 1197.45 \pm 0.04 \text{ MeV/c}^2 \text{ (34 ppm), and}$$

$$\mu_{\Sigma^-} = (-1.160 \pm 0.025)\ \mu_N \qquad (2.2\%).$$

For the magnetic moment there was introduced a significant error scale factor of 1.7 to take into account an appreciate disagreement between different previous experiments.

Crystal facility at FNAL Main Injector makes possible to improve by an order of magnitude a precision of the Σ^- mass and by a factor of two a precision of the Σ^- magnetic moment. The improved Σ^- mass and magnetic moment allow to study, at further, the Σ^- nucleus spin-orbit strong interaction and to measure the binding energy of the Σ^- n hypernucleus, if it exists (see next sections).

The most suitable transition for the measurement of the Σ^- mass and magnetic moment is the 5g-4f of Σ-C atom. The result of simulation is shown in Fig. 7. The estimated beam exposition is about 20 hours. Other suitable transition is the 6h-5g in oxygen (Fig.8).

2.4 Σ^- Spin-Orbit Strong Interaction with Nuclei

One of the goals of low energy strong interaction physics is to reach a consistent discription of *NN*, *YN* and *YY* interactions by taking into account the quark structure of the hadrons [17,18]. The point in theory where the quark degrees of freedom prove to be essential is the prediction for strength of spin-orbit interaction because of a short range of the latter [19,20].

Up to now only *NN* spin-orbit interaction was extensively studied, in fact. For *YN* and *YY* sectors of baryon-baryon interaction we have no experimental data except for measurements with Λ-

hypernuclei which led to conclusion that ΛN spin-orbit strength is much smaller than the NN one. At the moment theoretical models built to reproduce the experimental strengths of interaction of nucleons and Λ-hyperons lead to different predictions for other particles.

The theoretical calculations for Σ hyperon spin-orbit force are rather contradictory and changed from about zero up to 4/3 of nucleon force [21,22]. The recent calculations using relativistic σ–ω mean field theory with vertex couplings from quark model [23] led to the ratio of ΣN to NN spin-orbit interaction of about 1 which was used in our estimations (20 Mev for V_{LS} parameter of spin-orbit potential in notation of [21]).

Previously, the attempts to measure ΣN spin-orbit interaction were made at CERN, KEK, BNL, but no clear experimental data on this problem were obtained. The main difficulty is that Σ-hyperon should be unstable in nuclei due to fast $\Sigma N \rightarrow \Lambda N$ conversion. Its decay width in nuclear matter was estimated to be about 20 MeV that is much more than possible spin-orbit splitting in Σ-hypernuclei if they exist. The existence of Σ-hypernuclei is now suspected because of the all early observations of narrow Σ-hyper-nuclear states was not confirmed by latest measurements [24]. At the same time, a fast decay of hyperons prevents to carry out scattering experiments.

On the other hand, it is known, when the captured hadron occupies a lower atomic levels whose wave function have appreciable overlap with the nucleus, it undergoes a strong interaction with nucleons which results in shifts and broadens of atomic level energies with respect to electromagnetic values providing a way to study hadron-nucleon interaction alternatively to scattering and hypernuclei researches.

Early estimation of nuclear spin-orbit interaction in Σ-atoms was made in [25] where the 3d-2p transition in Σ-^{4}He atom was proposed to measure. However, according to our calculations the most suitable transition for measuring spin-orbit effect with proposed crystal facility at FNAL is the 5g-4f transition in Σ-O atom having transition energy of about 42.7 keV. Spin-orbit force changes splitting between components in comparison with a pure electromagnetic case, as shown in Fig.9. The result of simulation is shown in Fig.10, from which one can see that spin-orbit effect can be measured with accuracy of about several percents during several days.

2.5 Search for Σ^-n Hypernucleus

Searching for the simplest compound systems and studying their properties provide important information on the interactions involved. From this point of view the $\Sigma^- n$ hypernucleus is a promising object.

It was found in the previous studies that $\Sigma^- n$ interaction is weaker than p-n interaction, but any clear conclusion on existence, or nonexistence, of bound $\Sigma^- n$ state can not be done from available data. Different analyses [17,18] of measured cross-sections give more or less strong attraction in the singlet state of $\Sigma^- n$ (I=3/2), and weak attraction or even repulsion in the triplet state which is expected therefore to be definitely unbound. The calculated scattering length and effective force range in the singlet state of $\Sigma^- n$ is changed from -1 up to -5 fm and from 3 up to 10 fm, respectively. The uncertainties of the parameters are too large to conclude whether the bound state exists or not.

A bound $\Sigma^- n$ system was unsuccessfully searched for in K^- capture by D and ^{4}He at rest (for references see [26]). Later it was shown that production of $\Sigma^- n$ singlet state in K^-D capture is strongly suppressed and negative result is to be expected. For ^{4}He nucleus, the upper limit (1 event) was obtained [27] which is equal to about 0.3% per Σ^- produced in K^- ^{4}He capture. Other searches with K^- beams mentioned in [26] are unpublished. Just recently indication on bound $\Sigma^- n$ state in P-wave for reaction of 870 MeV/c K^- beam with ^{3}He target was reported, but statistics is insufficient for unambiguous conclusion [28].

If bound $\Sigma^- n$ system exists, then Σ^- hyperon may pickup a neutron from the nucleus where it was produced in inelastic proton-nucleon collision. This hypernuleus should have lifetime of about lifetime of Σ^- hyperon (due to a weak mode of decay $\Sigma^- n \rightarrow \pi^- + n + n$), therefore after leaving nucleus it may stop in matter and be captured onto atomic level, like other negative hadrons. So an

observation of the X-rays from the $\Sigma^- n$-atoms would be a clear signature of $\Sigma^- n$ hypernucleus existence.

Rough estimation of the pickup process probability can be done by comparison with (p,d) reaction. For protons with energy of tens MeV (it is the order of the initial kinetic energy of the Σ^- hyperons which can stop in the carbon target before decay) and for light nuclei the measured overall (p,d) cross-sections lie in the region 10-40 mb [29,30]. According to Baz' et al. [31] a cross-section depends on binding energy as $\sigma \sim \sqrt{\varepsilon}$. If we assume that the binding energy of $\Sigma^- n$ is in the region of 0.3 – 0.5 MeV [32] then a cross-section for Σ^- hyperon to pickup a neutron can be estimated as 5–20 mb providing the ratio of $\Sigma^- n$ atomic production to Σ^- atomic production of about several percents.

Encouraged by this estimation, we propose to search for the 6h-5g transition in $\Sigma^- n$-C atom having energy 21.1 keV. From this measurement, if line will be found, the spin and the binding energy of $\Sigma^- n$ bound state can be obtained. For example, a singlet structure of line corresponds to the singlet spin state of $\Sigma^- n$, the transition energy gives a value of the $\Sigma^- n$ mass, the binding energy $\varepsilon_{\Sigma^- n}$ of the $\Sigma^- n$ hypernucleus is calculated from the equation using known Σ^- hyperon and neutron masses:

$$m_{\Sigma^- n} = m_{\Sigma^-} + m_n - \varepsilon_{\Sigma^- n}.$$

The result of simulation for 3% ratio of $\Sigma^- n$ to Σ^- atomic production is shown in Fig. 11. The estimated accuracy of binding energy determination is about several percents for two-three weeks exposition.

2.6 Ξ and Ω Atoms

Our estimations of Ξ-atoms and Ω-atoms production have very large uncertainties and can be corrected if production rates of π, K, $\bar{p}$ and Σ atoms at the FNAL Main Injector will be measured.. The observation of Ξ-atoms would enable us to define prospects for studies with Ξ and Ω atoms, and specifically, for measuring Ω^- spin and electric quadrupole moment [33,34].

3. Experimental Setup

The main parts of the experimental setup are removable target station with replaceable targets, collimator mounted in the beam shielding, crystal spectrometer with crystal unit, and angle measuring system, and position sensitive X-ray detector, beam dump for secondary particles passing through collimator.

3.1 Principle of Operation

The source of the exotic atom's X-rays is a target bombarded by 120 GeV protons. Low energy negative particles produced in the target slow down and stop in it forming exotic atoms. The X-rays emitted by these atoms pass through a collimator mounted inside the shielding, are diffracted by a bent crystal to the focus, and detected. The beam of secondary particles passing through collimator is blocked by a beam dump. The energy of X-rays is found by measuring diffraction angle. The energy resolution of spectrometer are determined by quasimosaics of the bent crystal.

3.2 Crystal Spectrometer

The scheme of the Johansson (reflection type) spectrometer is shown in Fig.2, principle of double focusing is shown in Fig.3 The counting rate of the spectrometer for narrow lines is given by expressions:

$$n = V \cdot \frac{dN}{dV} \cdot Y \cdot k_{t\,\mathrm{arg}} \cdot \varepsilon_J ,$$

$$V \approx \frac{\pi d_{t\,\mathrm{arg}}^2}{4} \cdot \frac{b}{R} \cdot a,$$

$$\varepsilon_J = \frac{1}{4\pi} \cdot \frac{h}{(2R\sin\theta + a)} \cdot \frac{\omega R \sin\theta}{|a|} \cdot \Gamma \cdot k_{air} \cdot k_{crys} \cdot \varepsilon_{\mathrm{det}},$$

where

n - counting rate,
V - target volume seen by the crystal,
$\frac{dN}{dV}$ - particle stop's density in the volume V seen by the crystal,
Y - radiative yield of the transition, photon/particle stop,
k_{targ} - factor for X-ray absorption in the target,
ε_J - efficiency of Johansson spectrometer,
$d_{t\,\mathrm{arg}}$ - target diameter,
b - crystal size along focal circumference,
a - target displacement from spectrometer focus,
R - crystal bending radius,
h - crystal height,
θ - diffraction (Bragg) angle for incident X-rays,
ω - width of the crystal quasimosaics,
Γ - crystal reflection coefficient,
k_{air} - factor for X-ray absorption in air,
k_{crys} - factor for X-ray absorption in the crystal,
ε_{det} - detector efficiency.

The counting rate n is equal to the peak amplitude when measuring a reflection with step by step method using entrance slit in front of the detector (slit width is equal to $\omega R \sin\theta$). For measuring a reflection with multi-element detector (strip width $t_{strip} << \omega R \sin\theta$), the counting rate n is equal to the peak area.

Energy resolution ΔE of the spectrometer is determined by product of quasimosaics width ω and dispersion $\frac{dE}{d\theta}$:

$$\Delta E = \omega \cdot \frac{dE}{d\theta} = \omega \cdot \frac{2d_{hkl}E^2}{hc}\sqrt{1 - \left(\frac{hc}{2d_{hkl}E}\right)^2},$$

where

d_{hkl} - interplanar distance for the system of reflecting planes (hkl),
E - energy of incident X-rays,
h - Planck constant,
c - speed of light.

Background from the target can be calculated as follows:

$$n_b = 4\pi \cdot \frac{dN}{dEd\Omega} \cdot \frac{dE}{d\theta} \cdot \Delta\theta \cdot k_{targ} \cdot \varepsilon_C,$$

where n_b - background counting rate,

$\frac{dN}{dEd\Omega}$ - spectral density of photons produced in the target,

$\Delta\theta$ - angle width of the sensitive region along the focal circumference (slit width or strip width in case of multi-element detector).

The various cuts of crystal plate from a monocrystal have different interplanar distances d_{hkl}, quasimosaics width ω, and reflecting power Γ. The choice of appropriate cut provides the best conditions for measurement [35]. To fabricate the double focusing crystal unit a technology developed at PNPI will be used.

Crystal spectrometer requires about 40 × 40 ft^2 of a floor space enclosed to housing to provide stable temperature and humidity during experiment.

The length of beam target in beam direction is equal to 2 cm, diameter – 2 or3 cm.. The materials are C, BeO.

3.3 X-ray Detector

Double focusing is a very essential feature of the installation which allows to apply position-sensitive detector for measurements of diffraction spectra. A silicon multi-element detector with position resolution of 25 μm and energy resolution of about 1 keV increases setup efficiency by an order of magnitude when studying multi-component X-ray lines. Simultaneously, it decreases background and systematic error caused by beam instability during experiment.

We suppose that the detector can be done from high purity Si plate of ~2 mm thickness having a linear array of ~400 strips of ~40 × 0.025 mm^2 size. Previous studies in designing position-sensitive semiconductor detectors for X-rays testify a feasibility of this device . For soft X-rays a CCD detector can be used.

3.4 Calibration

Calibration of spectrometer can be done using MoK_α (17.4 keV) and AgK_α (22.1 keV) lines from X-ray tubes and antiprotonic 5g-4f line (18.7 keV) from carbon target.

3.5 Effect and Background

To estimate exotic atom production at FNAL Main Injector we used GEANT 3.21 with FLUKA [36] as a hadronic shower generator. The applicability of the simulation tools was tested by comparison with measurements at IHEP in which a reasonable agreement was achieved for both particle stops and low energy photon production.

Monte-Carlo results for carbon target are shown in Table 1 and Fig12. The length of target along proton beam is equal to 2 cm, diameter - 3 cm. In case of oxygen it is proposed to use BeO target which provides the production rates approximately the same as the carbon target.

The IHEP measurements show that the background of secondary particles passing through the collimator and channel shielding (first of all, neutrons and hard γ-rays) can be successfully suppressed by improving protection near detector and decreasing its sensitive volume. Additional suppression is provided by applying a position-sensitive detector. Therefore in all simulations, we neglected background from secondaries and took into account only bremsstrahlung from the target.

We suppose that beam intensity on the target is equal to 10^{13} protons per cycle, and slow extraction mode with 1s flattop is used.

3.6 Time Estimations

In Table 2 the measurements with crystal facility at FNAL MI are summarized including time estimations and anticipated results. Time estimations take into account adjustments and calibrations.

4. Acknowledgements

We are grateful to A.A.Vorobyev for initiating and supporting this work and to G.Bock, N.F.Bondar, C.Brown, J.Lach, N.Mokhov, O.E.Prokofiev, V.G.Razmyslovich, N.K.Terentyev for useful discussions and help during proposal preparation.

The project is supported by Russian Foundation for Basic Researches, grant 01-02-17992.

References

[1] A.S. Denisov, A.V. Zhelamkov, Yu.M. Ivanov, L.P. Lapina, P.M. Levchen-ko, A.A. Petrunin, A.G. Sergeev, A.I. Smirnov, V.M. Suvorov, and O.L. Fedin, JETP Lett., **54**, 558(1991)

[2] M.P. Gur'ev, A.S. Denisov, A.V. Zhelamkov, Yu.M. Ivanov, L.P. Lapina, P.M. Levchenko, A.A. Petrunin, Yu.P. Platonov, A.G. Sergeev, A.I. Smirnov, V.M. Suvorov, and O.L. Fedin, JETP Lett., **57**, 400(1993)

[3] V.I. Marushenko, A.F. Mezentsev, A.A. Petrunin, S.G. Skornyakov, and A.I.Smirnov, JETP Lett., **23**, 72(1976)

[4] F. Boehm, A. Hahn, H.E. Henrikson, J. Miller, R.J. Powers, P. Vogel, J.L. Vuilleumier, and K.C.Wang, Phys.Rev.Lett., **38**, 215(1977)

[5] L. Delker, G. Dugan, C.S. Wu, D.C. Lu, A.J. Caffrey, Y.T. Cheng, and Y.K. Lee, Phys.Rev.Lett, **42**, 89(1979)

[6] G. de Chambrier, W. Beer, F.W.N. de Boer, K. Bos, A.I. Egorov, M. Eckhause, K.L. Giovanetti, P.F.A. Goudsmit, B. Jeckelmann, K.E. Kir'yanov, L.N. Kondurova, L. Lapina, H.J. Leisi, V.I.Marushenko, A.F. Mezentsev, A.A. Petrunin, A.G. Sergeev, A.I. Smirnov, G. Strassner,V.M. Suvorov, A. Vacchi, and D. Wieser, Nucl.Phys.A, **442**, 637(1985)

[7] D.E.Groom et al. (Particle Data Group), Eur. Phys. Jour. C**15**, 1(2000)

[8] B. Jeckelmann, P.F.A. Goudsmit, and H.J. Leisi, Phys.Lett.B, **335**, 326(1994)

[9] S. Lenz et al., Phys.Lett., **B 416**, 50(1998)

[10] K. Assamagan, Ch. Bronnimann, M. Daum, H. Forrer, R. Frosch, P. Gheno, R. Horisberger, M. Janoush, P.-R. Kettle, Th. Spirig, and C. Wigger, Phys.Rev.D, **53**, 6065(1996)

[11] K.P. Gall, E. Austin, J.P. Miller, F. O'Brien, B.L. Roberts, D.R. Tieger, G.W. Dodson, M. Eckhau-se, J. Ginkel, P.P. Guss, D.W. Hertzog, D. Joyce, J.R. Kane, C. Kenney, J. Kraiman, W.C. Phil-lips, W.F. Vulcan, R.E. Welsh, R.J. Whyley, R.G. Winter, R.J. Powers, R.B. Sutton, and A.R. Kunselman, Phys.Rev.Lett., **60**, 562(1991)

[12] Gerald Feinberg and Leon M. Lederman, "The Physics of Muons and Muon Neutrinos", Ann.Rev.Nucl.Sci., **13**, 431(1963)

[13] P.H. Frampton and P. Vogel, "Massive Neutrinos", Phys.Rep., **82**, 339(1982)

[14] Cyrus M. Hoffman and Vernon D. Sandberg, "Mass Limits for the Muon Neutrino",In Snowmass 1982 Proceedings, Elementary Particle Physics and Future Facilities, 552(1982)

[15] Ching Cheng-rui and Ho Tso-hsiu, "On the Determination of Neutrino Mass - a Critical Status Report", Phys.Rep., **112**, 1(1984)

[16] R.M. Ryndin, Phys.Rep., **134**, 317(1986)

[17] P.M.M. Maessen, Th.A. Rijken, and J.J.de Swart, Phys.Rev.C, **40**, 2226(1989)

[18] B. Holzenkamp, K. Holinde, and J. Speth, Nucl.Phys.A, **500**, 485(1989)

[19] A. Valcarce, A. Buchmann, F. Fernandez, and Amand Faessler, Phys.Rev.C, **51**, 1480(1995)

[20] Xuemin Jin and Marina Nielsen, Phys.Rev.C, **51**, 347(1995)

[21] A. Bouyssy, Nucl.Phys.A, **381**, 445(1982)

[22] C.B. Dover, D.J. Millener, and A. Gal, Phys.Rep., **184**, 1(1989)

[23] J. Cohen and H.J. Weber, Phys.Rev.C, **44**, 1181(1991)

[24] Proceedings of 23d International Symposium, Tokyo, March 15-18, 1995

[25] L.N. Bogdanova, A.E. Kudryavtsev, and V.E. Markushin, Effects of nuclear spin-orbit interaction in light Σ –atoms, Preprint ITEP-88, Moscow, 1985

[26] B. Budick, Nucl.Phys.A, **329**, 331(1979)

[27] R.A. Burnstein, W.C. Cummings, D.L. Swanson, and V.R. Veirs, Phys.Rev., **177**, 1945(1969)

[28] H. Piekarz, talk at the Sixth Conference on Intersections of Particle and Nuclear Physics, Big Sky Montana, USA, May 26 - June 2, 1997

[29] S.A. Goncharov, Yu.I. Denisov, A.M. Mukhamedzhanov, E.A. Romanovsky, G.E. Valiev, I.R. Gulamov, T. Iskhakov, G. Ni, N.K. Timofeyuk, R. Yarmu-khamedov, V . Kroga, and V.A. Stepanenko, Journal of Nuclear Physics, **44**, 303(1986)

[30] J.R. Campbell et al., Nucl.Phys.A, **470**, 349(1987)

[31] A.I. Baz', Ia.B. Zel'dovich, and A.M. Perelomov, Rasseyanie, reaktsii i raspady v nerelyativistskoi kvantovoi mekhanike, 2nd edition, "Nauka", Moscow, 1971, p.333; transl.: Scattering, reactions and decays in nonrelativistic quantum mechanics, Jerusalem, Israel Program for Scientific Translations, 1969

[32] G.A. Snow, Phys.Rev., **110**, 1192(1958)

[33] S.P. Alliluyev, S.S. Gershtein, "On the Ω^- hyperon quadrupole moment and a possibility to measure it", preprint IHEP 78-111, Serpukhov, 1978

[34] S.S. Gershtein and Yu.M. Zinoviev, "On quadrupole moment of Ω^- hyperon", preprint IHEP 80-177, Serpukhov, 1980

[35] L.N. Kondurova and A.G. Sergeev, "The code for calculation of reflecting planes parameters for crystals used in crystal-diffraction spectrometer and for evaluation of diffraction spectra distortion due to multidiffraction", preprint PNPI-2087, Gatchina, 1995

[36] A. Fasso, A. Ferrari, J. Ranft, and P.R. Sala, "FLUKA: present status and future developments", Proceedings of the IV Int. Conf. on Calorimetry in High Energy Physics, La Biodola (Elba), September 19-25, 1993.

Table 1: Exotic atom's production at FNAL MI for carbon target.

Particle	Stops per proton
	C,(∅ 3cm × 2 cm)
μ^-	$3.5 \cdot 10^{-6}$
π^-	$1.3 \cdot 10^{-3}$
K^-	$2.7 \cdot 10^{-5}$
$\bar{p}$	$1.9 \cdot 10^{-6}$
Σ^-	$4.4 \cdot 10^{-6}$
Ξ^-	$1.0 \cdot 10^{-7}$
Ω^-	$\leq 2.0 \cdot 10^{-9}$

Table 2: Measurements with exotic atoms at FNAL MI.

Experiment	Transition	Exposition	Precision
π^- mass	π-O, 5f-3d, 16.8 keV	30 h	1 ppm
K^- mass	K-C, 4f-3d, 22.1 keV	20 h	1-2 ppm
Σ^- mass	Σ-C, 5g-4f, 23.4 keV	40 h	1-2 ppm
Σ^-N spin-orbit	Σ-O, 5g-4f, 42.7 keV	60 h	2%
Σ^- n search and mass	Σ^-n-C,6h-5g,21.1 keV	500 h	1-2 ppm

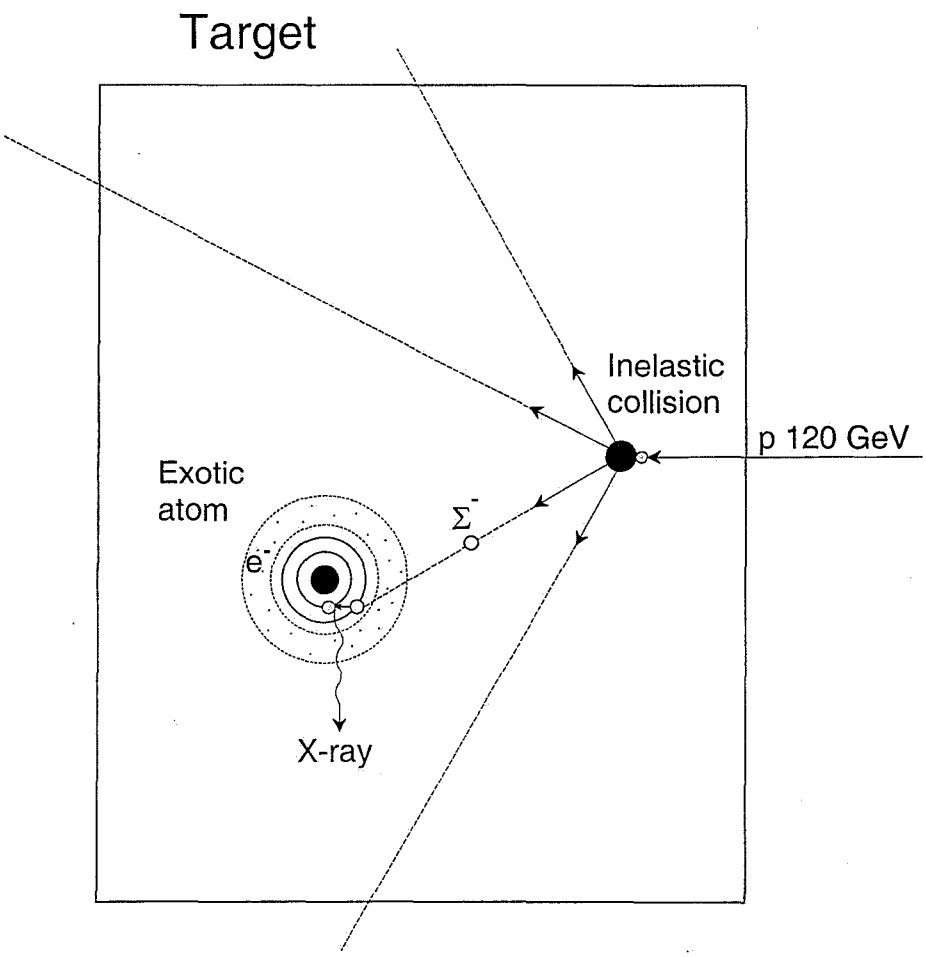

Figure 1. Production of exotic atoms in target.

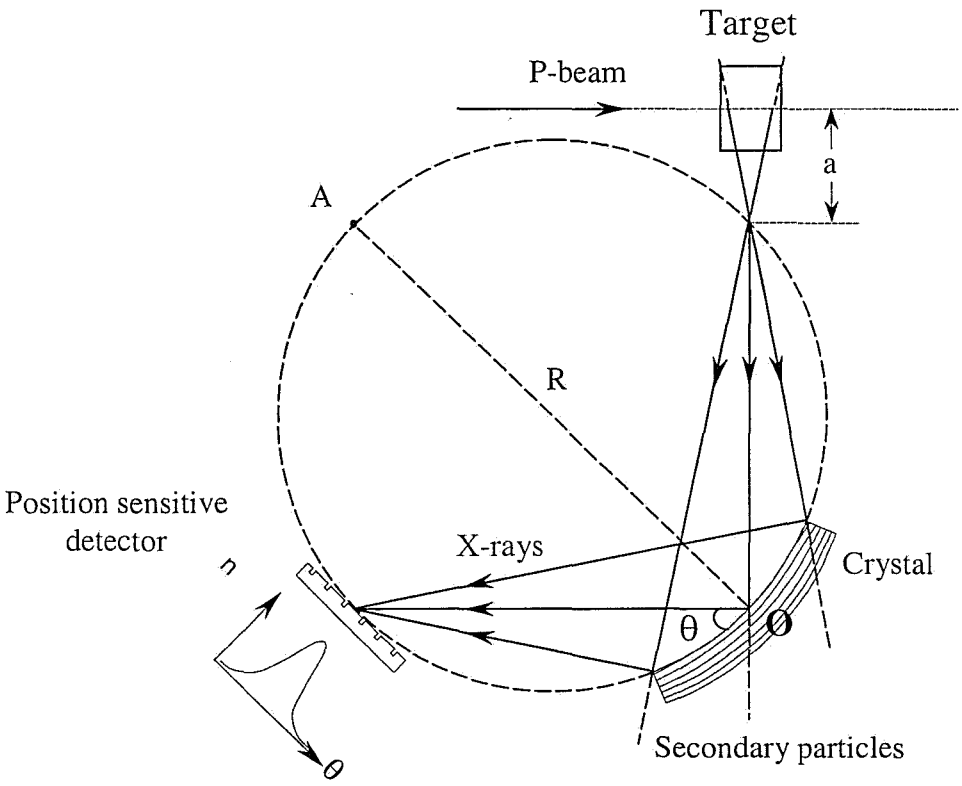

Figure 2. Principal scheme of Johansson spectrometer.

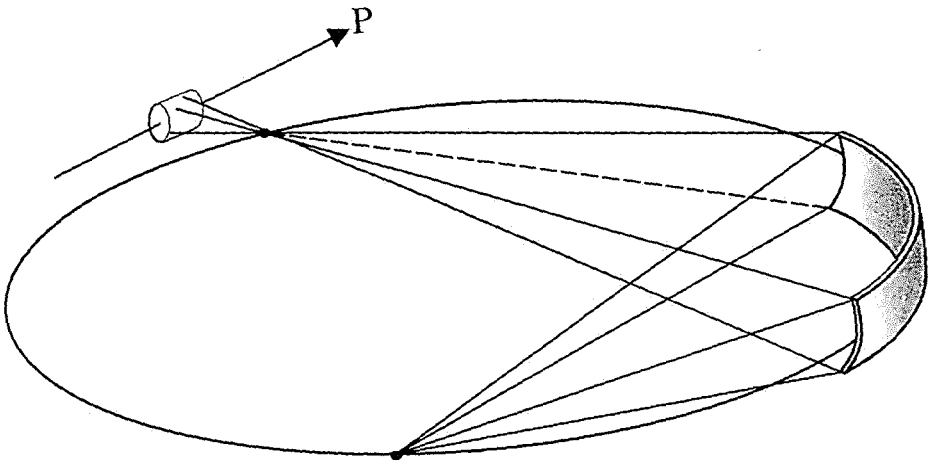

Figure 3: Principle of double focusing with toroidal bent crystal.

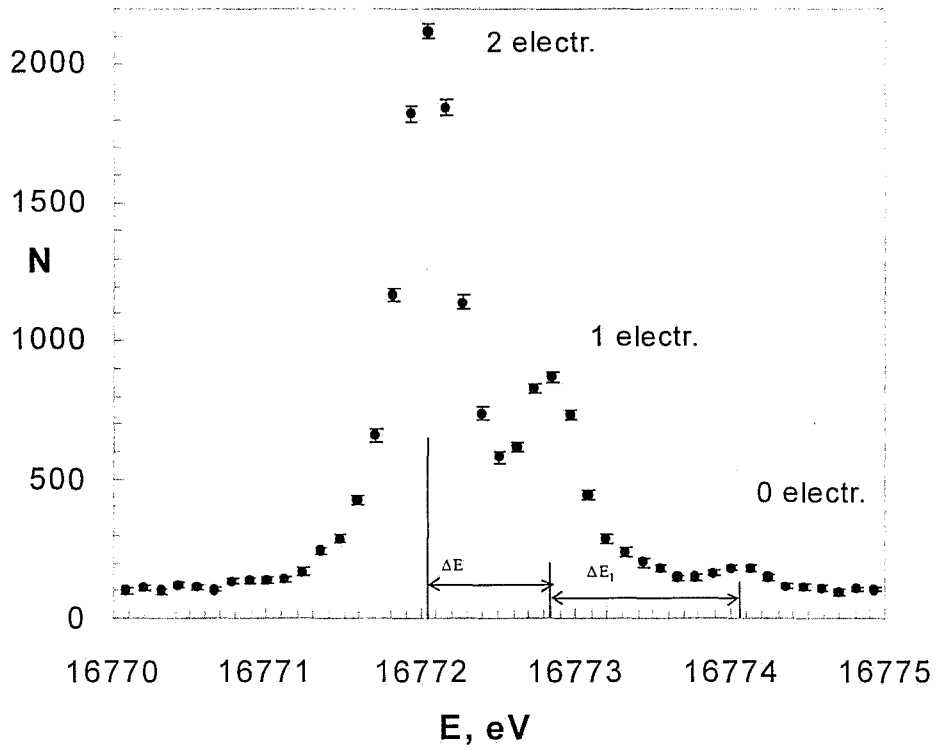

1 Monte-Carlo simulation for Johansson spectrometer

Target : BeO , diameter 2 cm , length 2 cm

Detector : Si, multi-element, thickness 2 mm,
position resolution 25 μm

Statistics : 10 hour with 10**13 protons per 3 seconds

Energy (angle) resolution : 0.35 eV (3.0 arcsec)

$\Delta E = 0.7996 \pm 0.0064$ eV

$\Delta E_1 = 1.210 \pm 0.032$ eV

$E_{5f\text{-}3d} = 16772.0422 \pm 0.0029$ eV (0.18 ppm)

Figure 4. MC simulation for π^- mass measurement at FNAL MI.

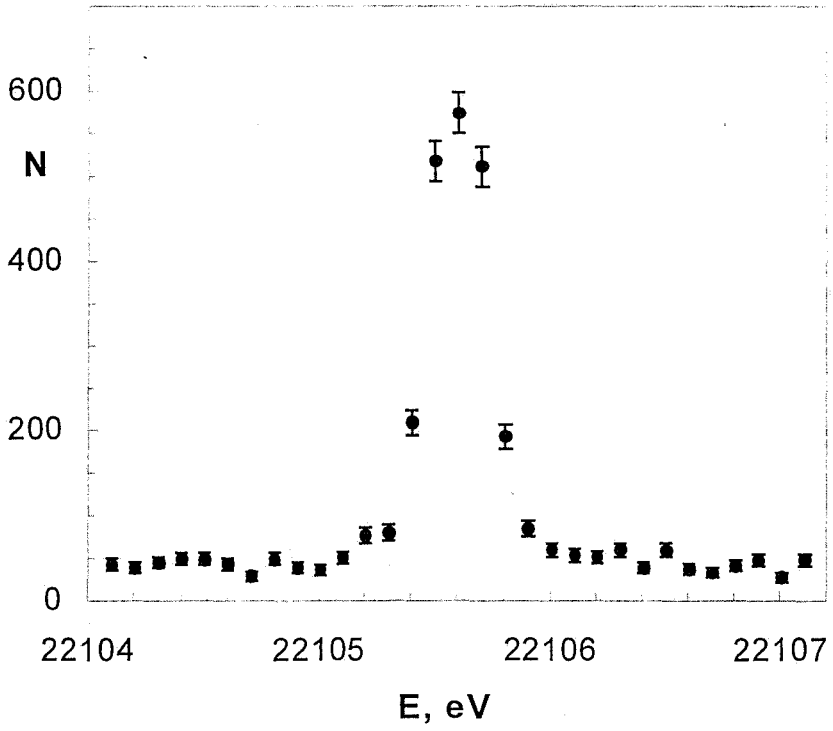

2 Monte-Carlo simulation for Johansson spectrometer

Target : C , diameter 3 cm , length 2 cm

Detector : Si, multi-element, thickness 2 mm,
position resolution 25 μm

Statistics : 3 hour with 10**13 protons per 3 seconds

Energy (angle) resolution : 0.95 eV (3.3 arcsec)

$E_{4f\text{-}3d}$ = 22105.6050 ± 0.0035 eV (0.16 ppm)

Figure 5: MC simulation for $\bar{K}$ mass measurement with carbon at FNAL MI.

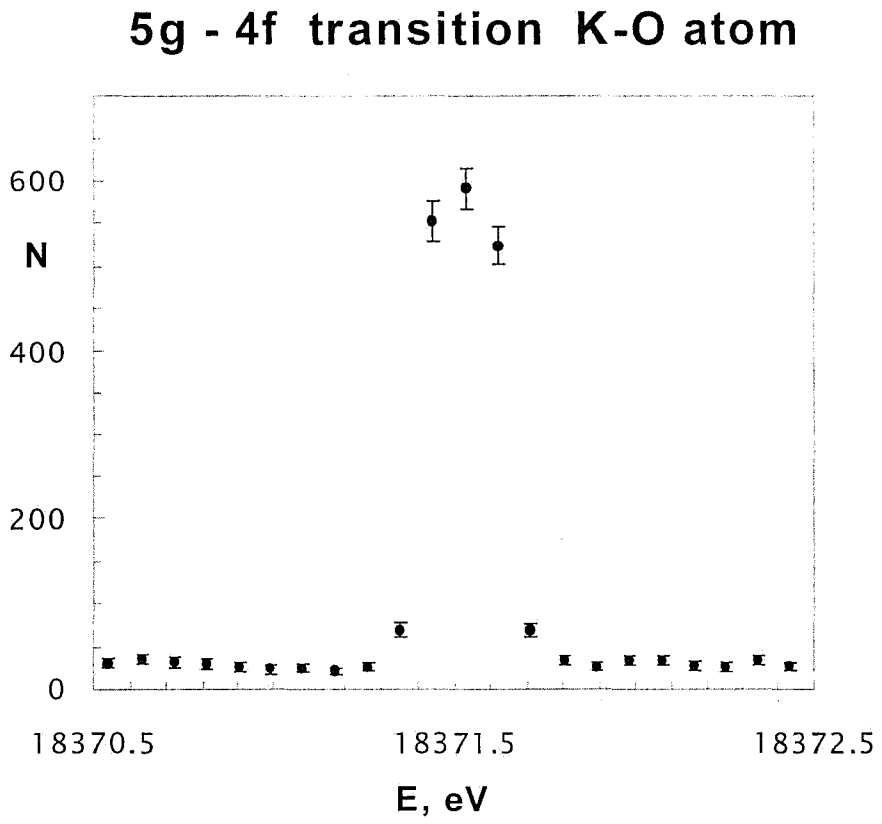

Monte-Carlo simulation for Johansson spectrometer

Target : BeO , diameter 2 cm , length 2 cm

Detector : Si, multi-element, thickness 2 mm,
position resolution 25 μm

Statistics : 3 hour with 10**13 protons per 3 seconds

Energy (angle) resolution : 0.28 eV (3.0 arcsec)

$E\ 5g_{-4f}$ = 18371.5320 ± 0.0020 eV (0.11 ppm)

Figure 6: MC simulation for $\bar{K}$ mass measurement with oxygen at FNAL MI.

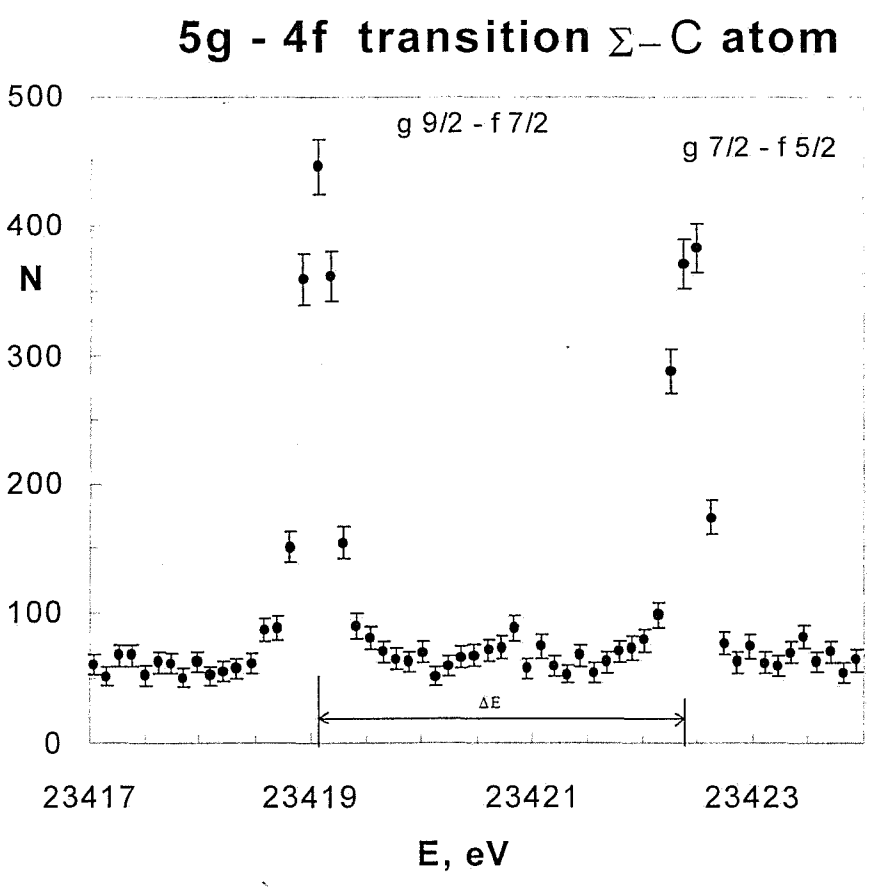

3 Monte-Carlo simulation for Johansson spectrometer

Target : C , diameter 3 cm , length 2 cm

Detector : Si, multi-element, thickness 2 mm,
position resolution 25 mm

4 Statistics : 20 hours with 1013 protons per 3 seconds**

Energy (angle) resolution : 0.36 eV (3.0 arcsec)

ΔE = -3.3660 ± 0.0090 eV

$E_{5g\text{-}4f}$ = 23420.470 ± 0.0084 eV (0.36 ppm)

Figure 7. MC simulation for Σ^- mass and magnetic moment measurement with
carbon at FNAL MI.

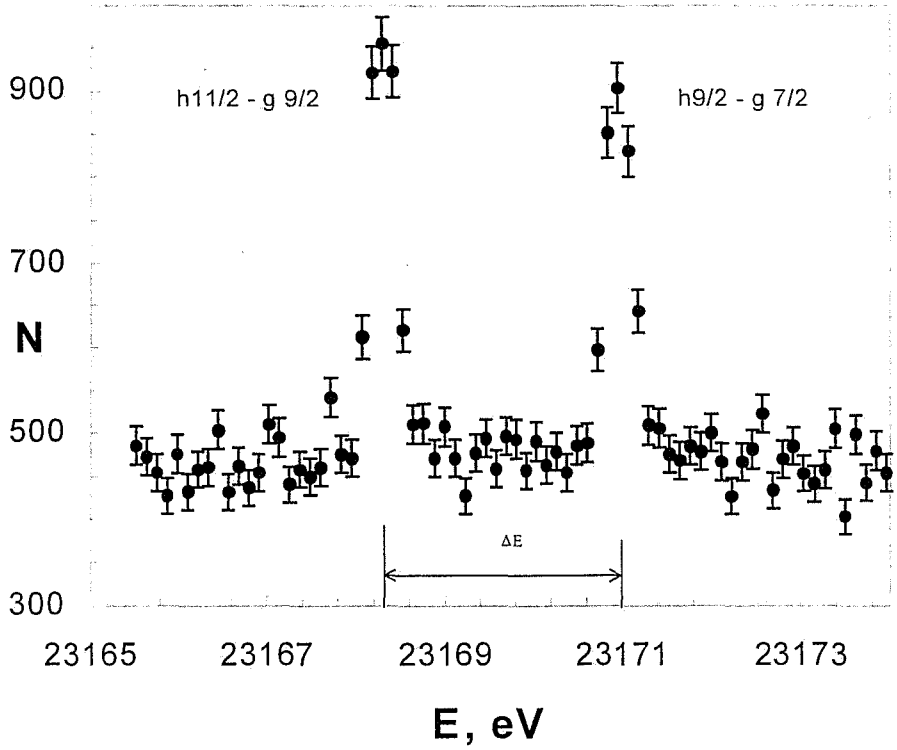

Monte-Carlo simulation for Johansson spectrometer

Target : BeO , diameter 2 cm , length 2 cm

Detector : Si, multi-element, thickness 2 mm,
position resolution 25 μm

Statistics : 20 hours with 10**13 protons per 3 seconds

Energy (angle) resolution : 0.35 eV (3.0 arcsec)

$\Delta E = -2.665 \pm 0.011$ eV

$E_{6h\text{-}5g} = 23169.465 \pm 0.068$ eV (0.29 ppm)

Figure 8: MC simulation for Σ^- mass and magnetic moment measurement with
oxygen at FNAL MI.

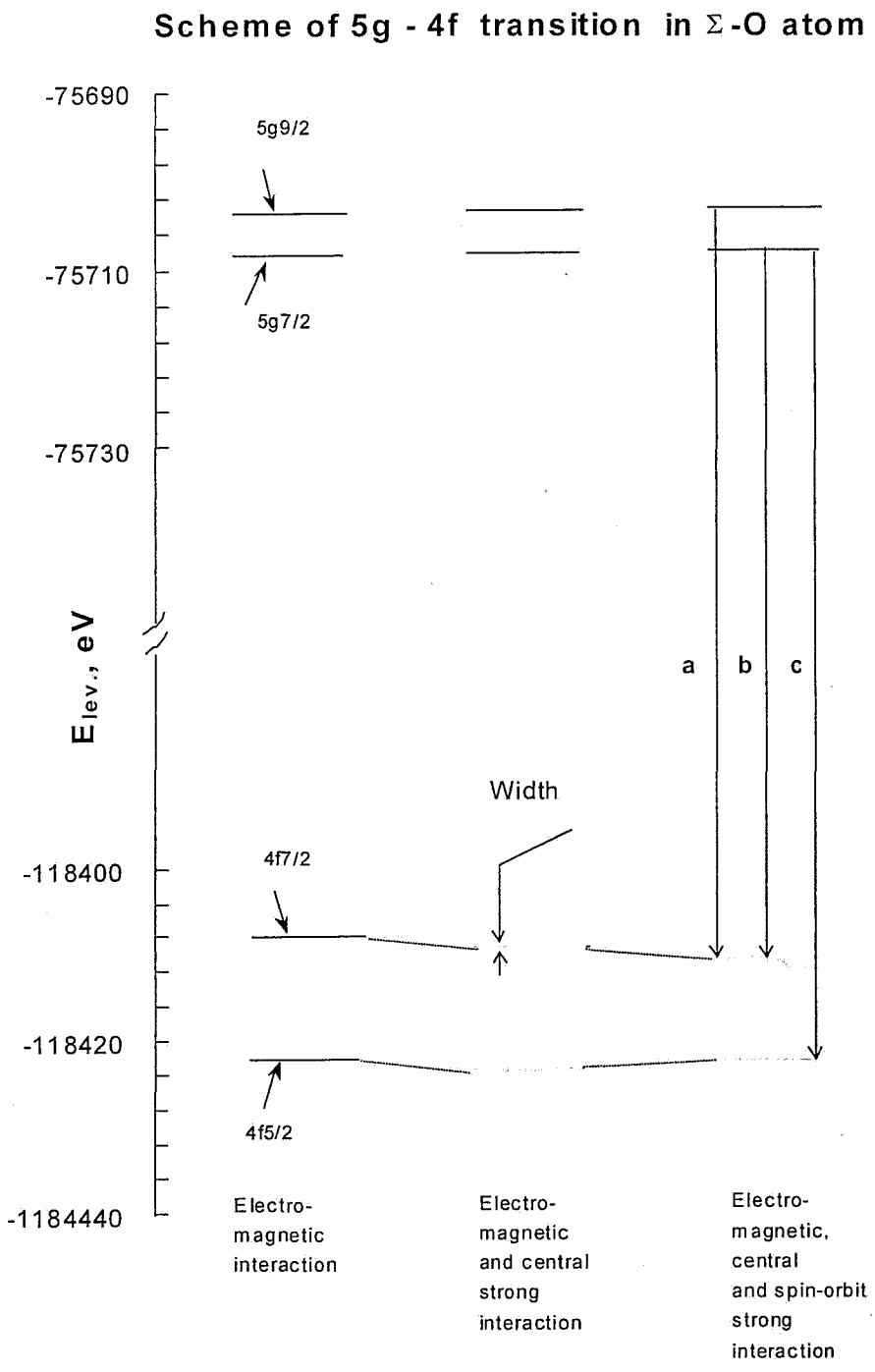

Figure 9. Fine structure of 5g-4f transition in the Σ-O atom.

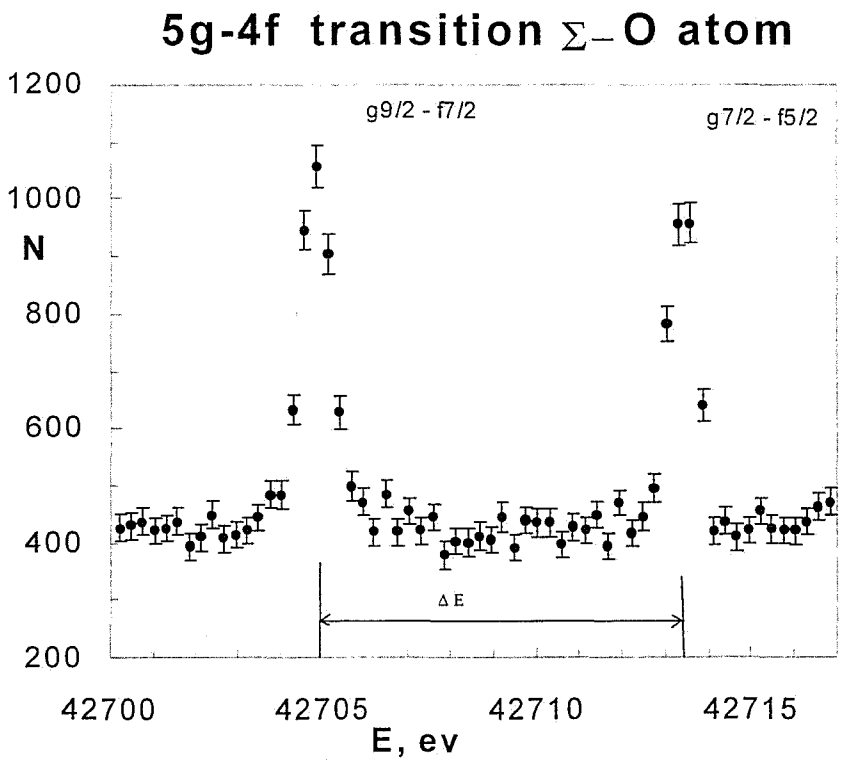

Monte-Carlo simulation for Johansson spectrometer

Target : BeO , diameter 2 cm , length 2 cm

Detector : Si, multi-element, thickness 2 mm,
position resolution 25 μm

Statistics : 50 hours with 10**13 protons per 3 seconds

Energy (angle) resolution : 0.82 eV (3.0 arcsec)

$$\Delta E \quad \begin{cases} -8.548 \pm 0.019 \text{ ev} & V_{Ls} = 20 \text{ MeV} \\ -9.890 \text{ ev} & V_{Ls} = 0 \text{ MeV} \end{cases}$$

$E_{5g\text{-}4f}$ = 42708.446 ± 0.014 eV (0.34 ppm)

Figure 10. MC simulation for Σ^- nucleus spin-orbit force measurement at FNAL MI.

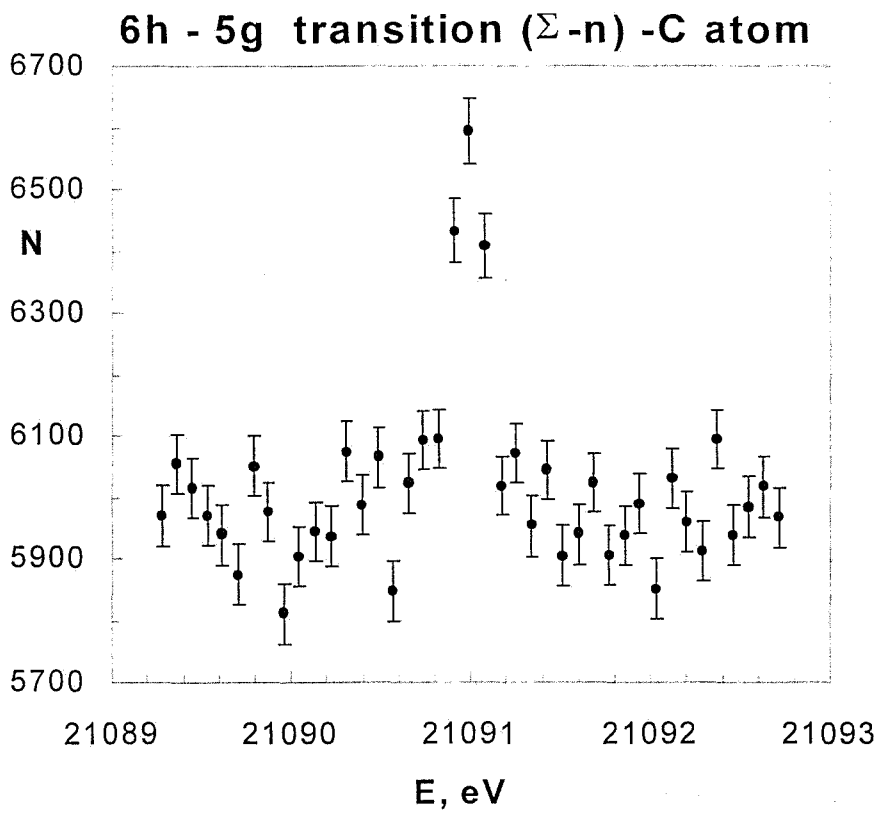

Monte-Carlo simulation for Johansson spectrometer

Target : C , diameter 3 cm , length 2 cm

Detector : Si, multi-element, thickness 2 mm,
position resolution 25 μm

Statistics : 500 hours with 10**13 protons per 3 seconds

Energy (angle) resolution : 0.26 eV (3.0 arcsec)

$E_{6h\text{-}5g}$ = 21091.000 ± 0.014 eV (0.68 ppm)

ε_b = 0.500 ± 0.011 MeV

Amplitude = 560 ± 50

Figure 11: MC simulation for (Σ^-n) mass measurement at FNAL MI.

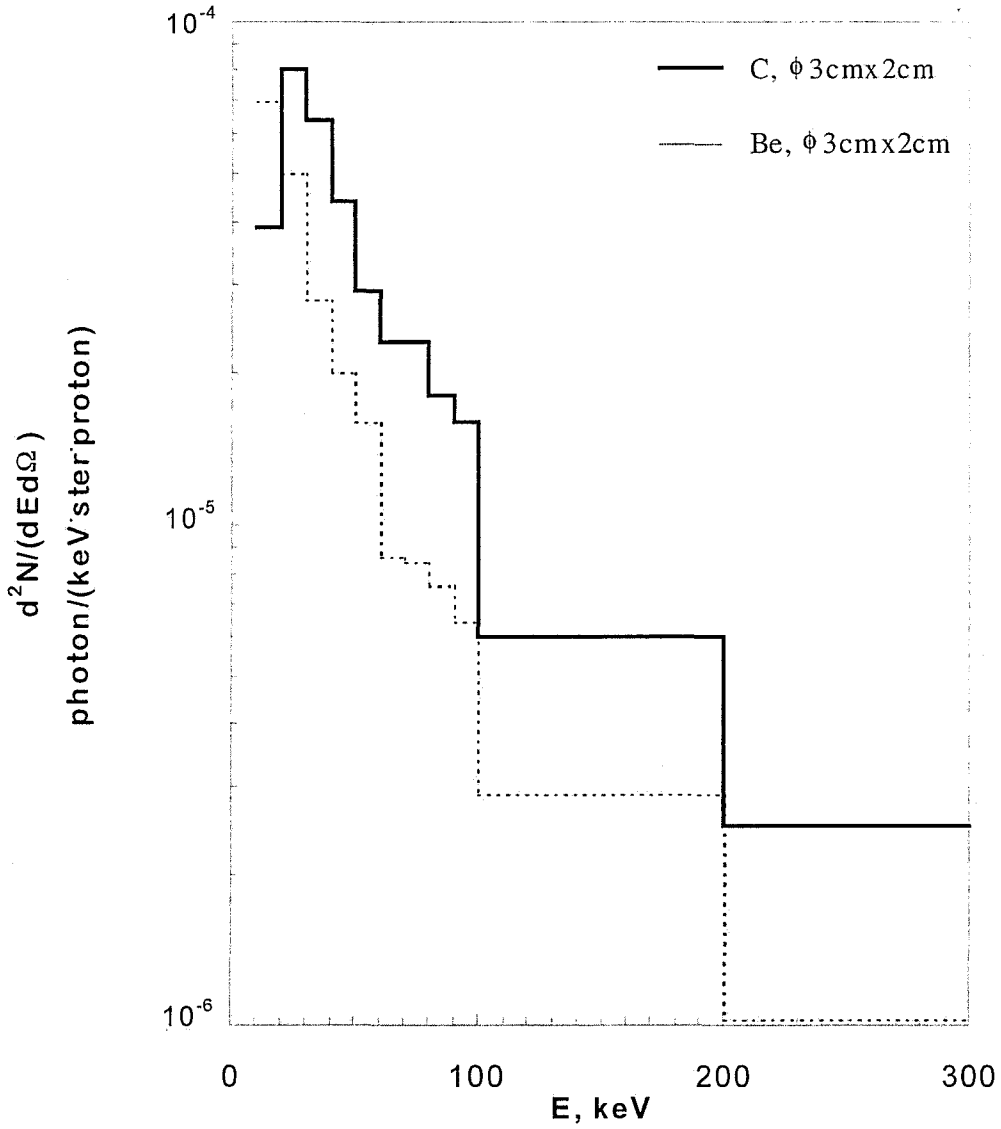

Figure 12. Photon production from Be and C targets at FNAL MI.